Lasers in Manufacturing Conference 2023

Process temperature measurement in the production of metal oxide layers by fast IR-detector

Alexander Nikolai Kaiser[a], Max-Jonathan Kleefoot[a,*], Eliene Olivera[a,b] , Harald Riegel[a]

[a]*LaserApplikationCenter (LAZ),Aalen University, 73430 Aalen, Germany*
[b]*Federal University of Vicosa, Viçosa 36570-900, Brazil*

Abstract

A variety of temperature-critical processes can be realized with laser material processing. For example, material surfaces can be functionalized by micro structuring with suitable parameter selection and processing strategies. Especially in the field of functional surfaces for tribological, optical, or biological applications micro structuring is versatile.
Further functionalization of the surface is the targeted heating to produce temper colors. The surface is heated locally, creating an oxide layer that develops a specific color when exposed to light. This process is known as laser coloring. In the latest literature, mainly the color and material changes related to the laser parameters were analyzed.
In this work, we want to analyze the process of laser coloring with a fast infrared detector. With the help of the detector, it should be possible to establish a correlation between the used laser parameters, the material, the produced color, and the measured infrared signal.

Keywords: Laser; micro structuring; surface functionalized; laser coloring; temperature measurement

1. Introduction

The use of stainless steel is a common practice in industry. The shimmering surface provides a visually good impression, and the corrosion resistance prevents the material from deterioration. Therefore, stainless steel is increasingly used for decorative purposes, such as in the automotive industry. However, the most common decorative use of stainless steel is in the construction industry (Harrison 2009; Nash 2005).

The appearance can be further changed by discoloring the stainless steel. This can be done by the generation of thin metal oxide layers on the surface of the material or with microstructures. The color of the

* Corresponding author. Tel.: +4973615762668
E-mail address: Alexander.Kaiser01@studmail.htw-aalen.de

metal oxide layers is determined by the way light interacts with the oxide layer. For non-iridescent colors, some light is reflected and some is absorbed on the surface of the oxide layer (Alliott et al. 2023).
The physical effect that produces the color of iridescent metal oxide films is thin-film interference. Thin film interference occurs when light waves reflected from the top and bottom of a thin film interfere with each other, resulting in constructive or destructive interference. The outcome is a change of the reflected light, which can lead to different colors. The thickness of the oxide layer determines the wavelength of the reflected light and thus the color that is observed (Panjan et al. 2014).
Another effect that contributes to the color of stainless steel is diffraction. Diffraction occurs when light waves are scattered by the microscopic structures, creating interference patterns that produce different colors. The spacing of the structures determines the diffraction grating and thus the wavelengths of light that are diffracted (Ahsan et al. 2011).

There are various processes for producing metal oxide layers on stainless steel. These can be divided into three categories: Electrochemical or non-electrochemical processes and laser coloring. In electrochemical processes, an electrolyte is used to either modify the existing chromium oxide layer on the stainless-steel surface or to deposit a completely new layer on top of the existing oxide. Non-electrochemical processes use media other than an electrolyte, such as high temperatures in thermal tinting and evaporation followed by condensation in physical vapor deposition (PVD) (Alliott et al. 2023). In the process of laser coloring, both electrochemical and non-electrochemical processes are possible. The discoloration of alloy steel by laser was first introduced by Maeda in 1987 in the patent “Method of improving functions of surface of alloy steel by means of irradiation of laser beam”. The material was placed in an oxidizing solution of acid or metallic salts and the Co2 laser was focused on the surface of the material. Due to the addition of the oxidizing solution, this is an electrochemical process.

In today's literature (Veiko et al. 2014; Liu et al. 2019; Li et al. 2009; Zheng et al. 2002), mainly non-electrochemical processes are used. Here, the laser is used as a heat source, with gaseous environment (O2 or N2 - also possible with atmospheric environment) contributing to the formation of the oxide layer. A main aspect which is crucial for the formation of the oxide layer is the temperature. Due to this, precise temperature control is essential to ensure optimum quality and uniformity of the oxide layer. In recent years, fast IR detectors have become a popular and effective temperature measurement technique. These detectors offer several advantages over conventional contact-based temperature measurement techniques, like high measurement speeds, or excellent spatial resolution (Rogalski 2002).

2. Experimental Setup

In the following chapter the experimental setup such as the parameter study, the imaging of the generated colors and the measurement setup are described more in detail.

2.1. Formation of oxide layer

At the beginning, the corresponding temperatures must be assigned for the colors. In the production of oxide layers on AISI304 stainless steel, suitable temperatures are found during heat treatment. Therefore, we used the colors and corresponding temperatures of the following authors.

Jerzy Labanowski investigated the heat discoloration of AISI 304 during welding and obtained the following temperatures for the respective colors (Table 1) (Łabanowski und Głowacka 2011).

These temperatures and colors are like those given by the British Stainless-Steel Association, with the difference that at 420 degrees purple/brown is produced instead of red brown, and at 450 degrees dark purple instead of dark red (British Stainless Steel Association 2023).

The eight colors, which range from yellow to dark blue/black, serve as a reference for the following investigations. To subsequently create the colors on a stainless steel sheet with 1,5mm thickness, the nanosecond laser from TRUMPF "TruMark 5020" with a maximum average power of 20 W, a scanner, and a F-Theta lens with a focal length of 160mm is used in combination with the "TruMark Station 5000". A preliminary investigation was carried out in which a wide range of parameters was examined. Promising parameter combinations were further used as the basis for the experimental plan.

Based on a parameter with the appropriate color, a parameter study was carried out. By varying the feed rate as well as the focus position, it was possible to create a change in color. From this parameter study, the following eight colors were chosen for the following investigations (Table 1).

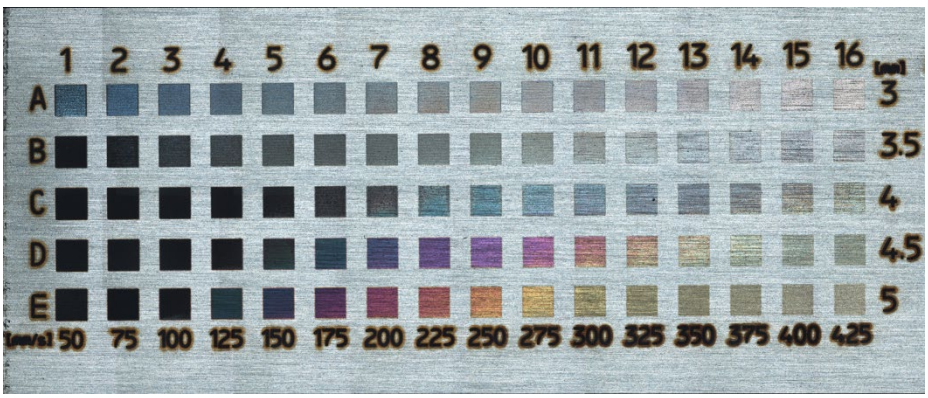

Fig. 1. Result of the Parameter study

Table 1: Temper color parameters

Color	Temperatures [°C]	Scan speed [mm/s]	Power [W]	Defocus [mm]	Frequency [kHz]	Puls duration [ns]	Hatch [µm]
Light Straw	290	420	20	5	224	30	50
Yellow Straw	340	320	20	5	224	30	50
Dark Yellow	370	275	20	5	224	30	50
Brown	390	250	20	5	224	30	50
Purple and Brown	420	225	20	5	224	30	50
Dark Purple	450	165	20	5	224	30	50
Blue	540	125	20	5	224	30	50
Black	600	75	20	5	224	30	50

2.2. Imaging of the generated temper colors

There are several methods for analyzing colors. One is the classical optical investigation with the help of a light microscope. Another one would be for example the spectral analysis. Higginson et al., for example, uses color spectrography to observe color development during the process and an optical microscope to image the

colors (Higginson et al. 2015). In this work, the colors are investigated with the help of an Axio Zoom optical microscope from ZEISS.

The colors can be depicted as follows:

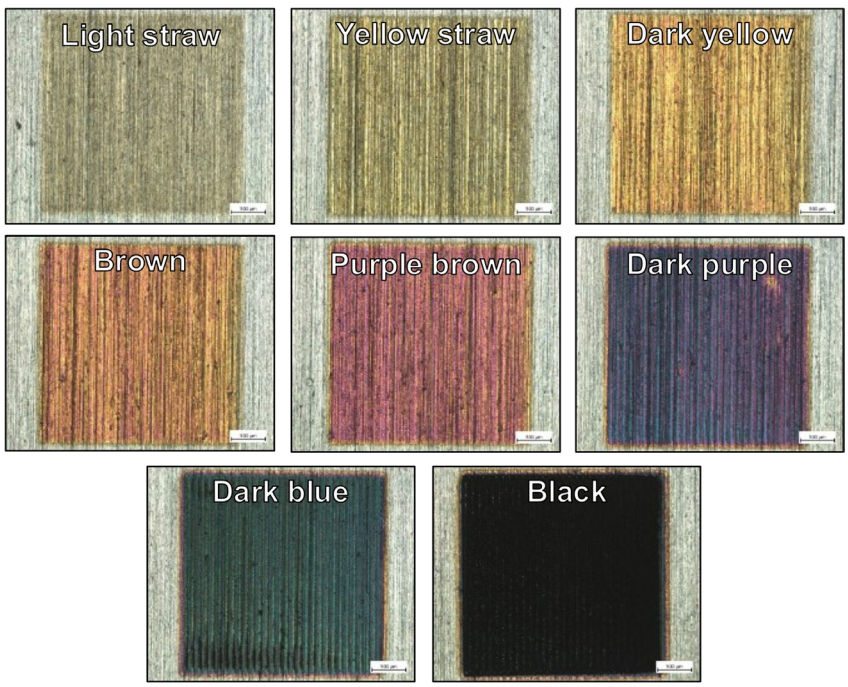

Fig. 2. Capture of the colors created by the parameters.

2.3. Measuring the produced temper colors

The measurement of the temperature during the laser coloring process is done with the help of a fast IR detector. This was also used by Martan et al. to measure temperatures during laser engraving (Martan et al. 2021; Martan et al. 2007; Martan et al. 2019). The used detector was a HgCdTe photodetector which observes an area of about 0.5 mm in diameter at an acquisition rate of 5 MHz. This makes it possible to detect and resolve signals even in very short time windows - as they often occur in laser processes - with the lowest possible time resolution in the range of 32 ns. Consequently, with the help of this detector it is possible to measure the temperature rise of each parameter set individual.

The measurement setup follows the schematic below:

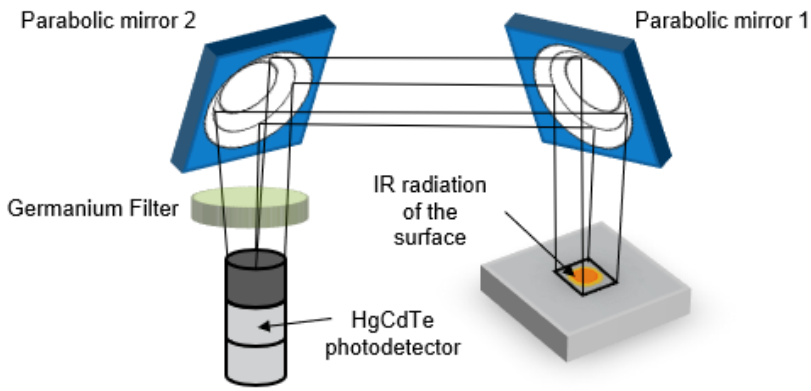

Fig. 3. Schematic representation of the measurement setup

The IR radiation of the process is guided from the surface by using two parabolic mirrors through a germanium filter and onto the detector. The signal thereby was recorded with an oscilloscope.

3. Algorithm of heat detection

At the beginning of each measurement, the noise of the base signal was recorded, with the lowest signal representing the value of the base characteristic U_b (Fig. 4 a). Then, the signal from the photodetector was recorded while the laser beam was coloring the surface of the processing fields. Due to the rather slow process, several line edits are performed to a field in the measurement area, which can be seen in Figure 4 a.

a)

b)

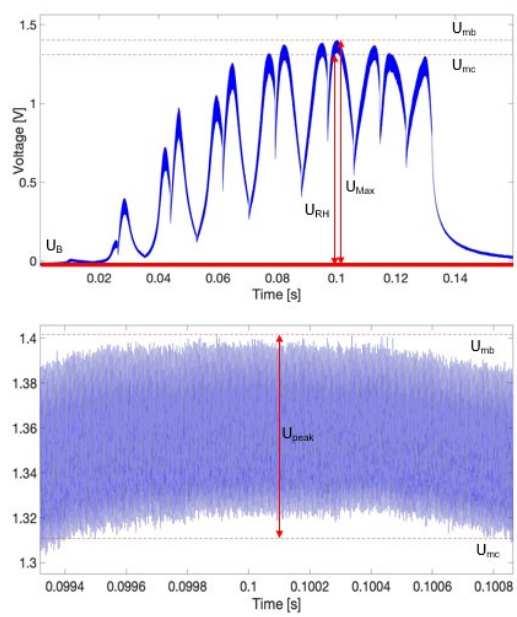

Fig. 4. Determination of the heat accumulation: a) - determination of the maximal signal U_{max} and the residual heat U_{RH}; b) - determination of the peak signal U_{peak}

The signal recording takes place in a 140 ms time window. The detection of the residual heat takes place within the hatching line which has the highest value. This hatching line is in a time window of about 15 ms. This is the part of the signal at which the process temperature is reached, and the process stabilizes. The remaining quantities of the algorithm can be determined from the measurement curve a). The software "WaveStudio" of the company Teledyne LeCroy already offers the possibility of an evaluation of the measuring signal by means of "peak to peak measuring". This possibility was also used and the maximum voltage U_{Max} was calculated as the difference between the noise U_B and the maximum measured voltage U_{mb}.

$$U_{Max} = U_{mb} - U_B \quad (1)$$

The points U_{mb} and U_B as well as the following point U_{mc} are not indicated as a number, but only used by the software "WaveStudio" for the evaluation. Likewise, the heating per pulse U_{peak} can be determined thereby. It represents the difference between the maximum measured voltage U_{mb} and the minimum measured voltage U_{mc} within a hatching line (Fig. 4 b).

$$U_{peak} = U_{mb} - U_B \quad (2)$$

As a result, the values of the distance U_{Max} and U_{peak} from Figure 4 are obtained, which are used for further calculations. The further calculations include the detection of the residual heat. Using the peak voltage U_{peak}, the residual heat U_{RH} can be determined as the difference between the maximum voltage U_{Max} and the peak voltage U_{peak}.

$$U_{RH} = U_{Max} - U_{peak} \quad (3)$$

4. Experimental Results

In the following Chapter the experimental results such as the observed color shift, the influence of the Line energy and the Feed rate are presented in more detail.

4.1. Shifting colors

After the series of tests had been carried out, it was first examined how the colors created during the measurements corresponded to the desired colors. It was found that the parameters used lead to a shift in the color gradient. The reason for this is that during the measurement a significantly smaller field of approx. 0.5 x 0.5mm^2 was processed. This leads to a higher heat accumulation between the individual hatching lines, which in turn leads to the colors shifting to higher temperatures. Due to the temperature shift, the parameters were assigned based on their colors. Due to the reassignment of the parameters, only 5 of the original 8 colors could be produced.

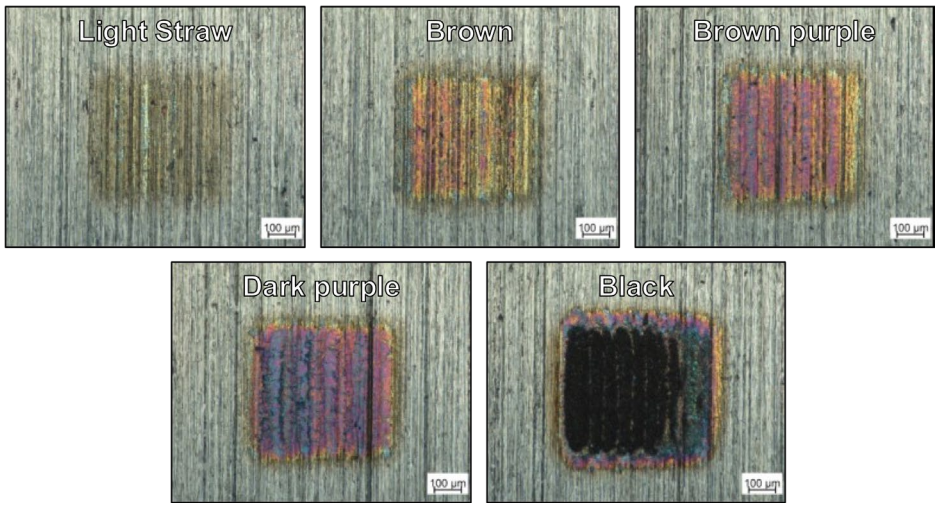

Fig. 5. Capture of the colors created by the parameters, during the measurement. Color shift during the heat accumulation in a smaller processing field

4.2. Influence of line energy

The line energy is the first parameter which is set in correlation to the voltage. The line energy describes the energy input per line in J/m. In comparison, the measured voltage increases almost exponentially with increasing line energy. The energy per unit length is directly related to the feed rate ($E = P_m/v_s$). Thus, the energy per unit length approaches the x-axis asymptotically, which means that the energy per unit length approaches zero with increasing feed rate. Due to the correlation, it can be said that from a line energy below 0,09 J/m the voltage increases nearly linear, above 0.09 J/mm, there is an exponential increase in voltage (See Figure 6).

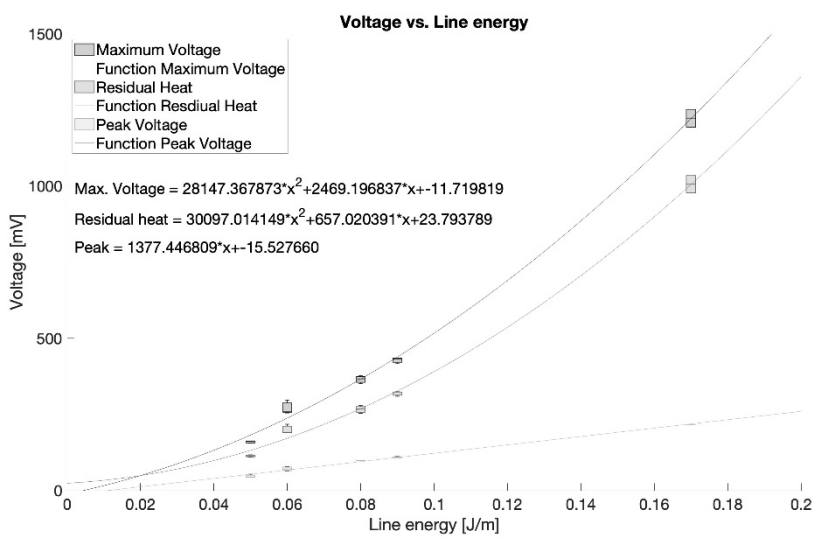

Fig. 6. Voltage over line energy

4.3. Influence of feed rate

When observing the voltage over the feed rate (Fig. 7), it becomes apparent that the voltage decreases with increasing feed rate. The values approach the x-axis asymptotically with increasing feed rate and follow the course of a hyperbola. The course of a hyperbola can also be seen during the line energy over the feed rate, whereby a dependency between the average power and the feed rate, as well as the voltage becomes apparent.

The single pulse fluence was chosen so low that the heat accumulation is necessary to generate the desired temperature. Increased heat accumulation can be achieved by varying the feed rate. The voltage of the heat accumulation increases significantly in the range < 225 mm/s. This suggests that parameter sets with feed rates < 225 mm/s are strongly influenced by heat accumulation. Consequently, there is a rapid increase in voltage, which is also accompanied by a color change. Based on this, it can be said that to produce tempering colors, the feed rate > 225 mm/s should be selected to keep the influence of heat accumulation as low as possible. To still produce the desired colors, the other parameters are adjusted in such a way that the single pulse fluence increases, but the heat accumulation remains low due to the high feed rates.

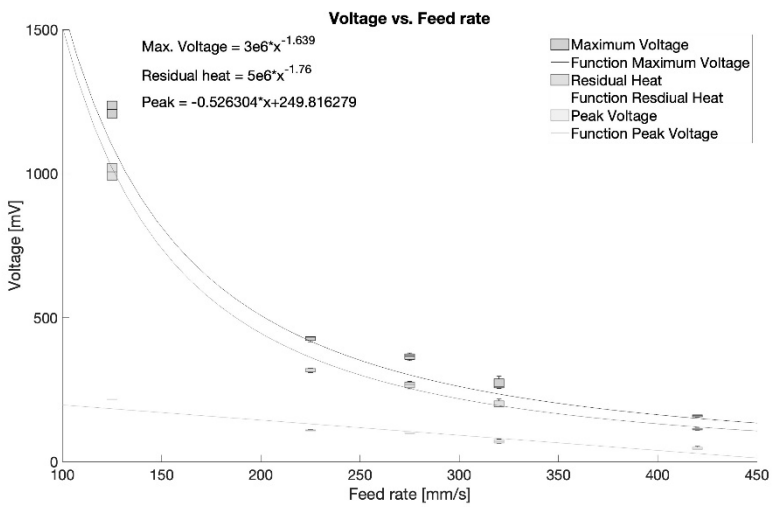

Fig. 7. Voltage over feed rate

4.4. Voltage and Temperature

When plotting the voltage as a function of temperature, the voltage increases almost linearly with increasing temperature. This behavior has also been observed for the line energy and indicates that the voltage increase is proportional to the temperature. By this comparison a calibration of the measurement setup seems to be possible. By converting the measured voltage values, the absolute temperatures during the process are obtained. The absolute temperatures are calculated using the formula $T = U*k$, where k stands for the calibration factor. The calibration factor is determined from the linear equation and represents its slope. However, since the structure has several degrees of freedom, the calibration is difficult, because it is only valid as long as the structure remains identical. For these reasons, only relative voltage values were considered in this work.

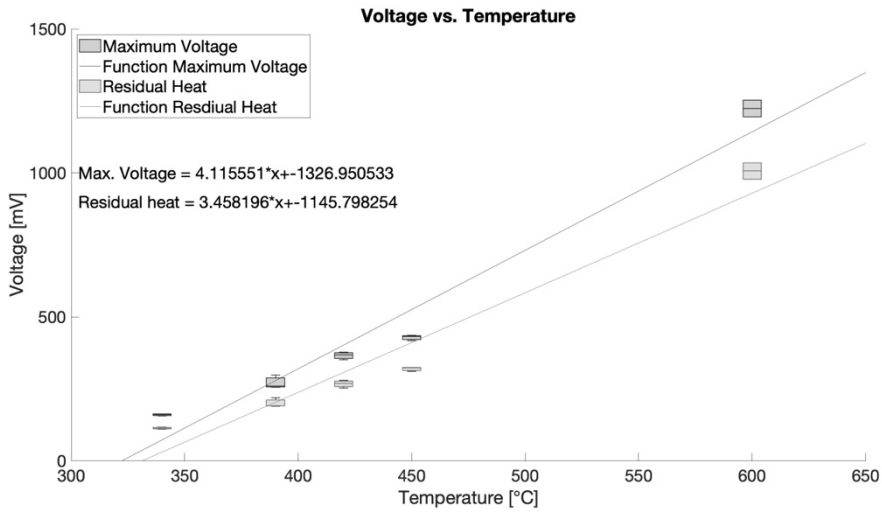

Fig. 8. Voltage over temperature for a determination of the calibration curve for absolute temperature calculation

5. Conclusion

In the present study, temperature during laser coloring was investigated. It could be determined that the used measurement setup is suitable for temperature monitoring during laser coloring. It is possible to acquire signals with a high temporal and spatial resolution during the process. With subsequent conversion of the voltage values based on the acquired calibration lines, additional measurements of the absolute temperature can be realized. It was visible that the feed rate is a decisive factor in heat accumulation. Therefore, feed rates higher than 225 mm/s should always be used when selecting parameters. At feed rates lower than 225 mm/s, heat accumulation increases exponentially, making it difficult to achieve the desired temperature accurately. However, high feed rates result in lower heat accumulation. To still generate the necessary temperatures for the corresponding colors, the single pulse energy must be increased. Furthermore, the function only counts within the intended limits of 75 – 420 mm/s. feed rate. Therefore, further investigations outside the limits defined by us are reasonable. The extrapolation of the curve indicates that with increasing feed rate the residual heat in the material increases again. This contradicts the practice because with increasing feed rate there is no spatial overlapping of the single pulses anymore. For these reasons, the investigation would have to be conduct with feed rates > 500 mm/s.

Acknowledgements

The authors acknowledge Jiri Martan and the University of West Bohemia for providing the measuring system “LabIR Ultrashort”.

References

Ahsan, Md. Shamim/Ahmed, Farid/Kim, Yeong Gyu/Lee, Man Seop/Jun, Martin B.G. (2011). Colorizing stainless steel surface by femtosecond laser induced micro/nano-structures. Applied Surface Science 257 (17), 7771–7777. https://doi.org/10.1016/j.apsusc.2011.04.027.

Alliott, G. T./Higginson, R. L./Wilcox, G. D. (2023). Producing a thin coloured film on stainless steels – a review. Part 2: non-electrochemical and laser processes. Transactions of the IMF 101 (2), 72–78. https://doi.org/10.1080/00202967.2022.2154495.

British Stainless Steel Association (2023). HEAT TINT (TEMPER) COLOURS ON STAINLESS STEEL SURFACE HEATED IN AIR. Online verfügbar unter https://bssa.org.uk/bssa_articles/heat-tint-temper-colours-on-stainless-steel-surface-heated-in-air/ (abgerufen am 21.05.2023).

Harrison, Alan (2009). Understanding stainless steel. Online verfügbar unter https://bssa.org.uk/bssa_articles/bssa-understanding-stainless-steel-centenary-edition/.

Higginson, R. L./Jackson, C. P./Murrell, E. L./Exworthy, P. A. Z./Mortimer, R. J./Worrall, D. R./Wilcox, G. D. (2015). Effect of thermally grown oxides on colour development of stainless steel. Materials at High Temperatures 32 (1-2), 113–117. https://doi.org/10.1179/0960340914Z.00000000083.

Łabanowski, Jerzy/Głowacka, Maria (2011). Heat tint colours on stainless steel and welded joints. Welding International 25 (7), 509–512. https://doi.org/10.1080/09507116.2010.540837.

Li, Z. L./Zheng, H. Y./Teh, K. M./Liu, Y. C./Lim, G. C./Seng, H. L./Yakovlev, N. L. (2009). Analysis of oxide formation induced by UV laser coloration of stainless steel. Applied Surface Science 256 (5), 1582–1588. https://doi.org/10.1016/j.apsusc.2009.09.025.

Liu, Huagang/Lin, Wenxiong/Hong, Minghui (2019). Surface coloring by laser irradiation of solid substrates. APL Photonics 4 (5), 51101. https://doi.org/10.1063/1.5089778.

Martan, J./Prokešová, L./Moskal, D./Ferreira de Faria, B. C./Honner, M./Lang, V. (2021). Heat accumulation temperature measurement in ultrashort pulse laser micromachining. International Journal of Heat and Mass Transfer 168, 120866. https://doi.org/10.1016/j.ijheatmasstransfer.2020.120866.

Martan, J./Semmar, N./Boulmer-Leborgne, C. (2007). IR Radiometry Optical System View Factor and Its Application to Emissivity Investigations of Solid and Liquid Phases. International Journal of Thermophysics 28 (4), 1342–1352. https://doi.org/10.1007/s10765-007-0264-1.

Martan, Jiří/Moskal, D./Prokešová, L./Honner, M. (Hg.) (2019). Detection of heat accumulation in laser surface texturing by fast infrared detectors, Lasers in Manufacturing Conference 2019, München.

Meada, Shigeyoshi/Yamamoto, Masahiro/Omata, Hiroyasu/Okada, Hideya (1986). Method of improving functions of surface of alloy steel by means of irradiation of laser beam, and alloy steel and structure made by the method, Anmeldedatum: 02.06.1986, Japan.

Nash, Eric P. (2005). Manhattan Skyscrapers. New York, NY, Princeton Architectural Press.

Panjan, M./Klanjšek Gunde, M./Panjan, P./Čekada, M. (2014). Designing the color of AlTiN hard coating through interference effect. Surface and Coatings Technology 254, 65–72. https://doi.org/10.1016/j.surfcoat.2014.05.065.

Rogalski, Antoni (2002). Infrared detectors: an overview. Infrared Physics & Technology 43 (3), 187–210. https://doi.org/10.1016/S1350-4495(02)00140-8.

Veiko, Vadim/Odintsova, Galina/Ageev, Eduard/Karlagina, Yulia/Loginov, Anatoliy/Skuratova, Alexandra/Gorbunova, Elena (2014). Controlled oxide films formation by nanosecond laser pulses for color marking. Optics express 22 (20), 24342–24347. https://doi.org/10.1364/OE.22.024342.

Zheng, H. Y./Lim, G. C./Wang, X. C./Tan, J. L./Hilfiker, James (2002). Process study for laser-induced surface coloration. Journal of Laser Applications 14 (4), 215–220. https://doi.org/10.2351/1.1514222.